JOURNAL OF THE MECHANICAL BEHAVIOR OF BIOMEDICAL MATERIALS 64 (2016) 113–124

Available online at www.sciencedirect.com

ScienceDirect

www.elsevier.com/locate/jmbbm

Research Paper

Prediction of cyclic delamination lives of plasma-sprayed hydroxyapatite coating on Ti–6Al–4V substrates with considering wear and dissolutions

Yuichi Otsuka[a,*], *Daisuke Kojima*[b], *Yoshiharu Mutoh*[a]

[a]*Department of System Safety, Nagaoka University of Technology, 1603-1 Kamitomioka, Nagaoka-shi, Niigata 940-2188, Japan*

[b]*Graduate School of Mechanical Engineering, Nagaoka University of Technology, 1603-1 Kamitomioka, Nagaoka-shi, Niigata 940-2188, Japan*

ARTICLE INFO

Article history:
Received 30 May 2015
Received in revised form
18 July 2016
Accepted 21 July 2016
Available online 29 July 2016

Keywords:
Hydroxyapatite coating
Delamination
Wear
Dissolution
Interface fracture mechanics
Fatigue life prediction

ABSTRACT

This study aims at developing the prediction model of cyclic delamination lives of plasma-sprayed HAp coating on Ti-6Al-4V substrate by considering wear by interface contacts and dissolution effect by Simulated Body Fluid (SBF). Delamination of HAp coating can lead to loosening of implants stem and final failure *in vivo*. In the fracture mechanism of interfaces between HAp coating with Ti substrates, only adhesive strength (interracial tensile strength) or fatigue behavior by longitudinal cracking have been observed. Cyclic delamination mechanism by considering various loading modes and corrosion effect has not been revealed yet. The interface delamination rates by cyclic loading were much higher than those by static loading tests. The result clearly demonstrated that the interface demalination behaviors are dominated not by maximum stress, but by stress range. Surface profile measurement and SEM observation also demonstrated damages by interface contact or third body wear at delamination tips of HAp coating only in the cases of compressions. The mechanisms of acceleration on the delaminations are third-body wear or wedge effect by worn particles which increased mean stress level during cyclic loading. Cyclic loading tests under SBF also revealed that cyclic delamination lives were shortened probably due to crevice corrosion at interfaces. Dissolutions at the tips of delaminations were observed by SEM images under tensile loading condition in SBF. Linearly adding the effects of wear and dissolutions into Paris law could successfully predict the delamination lives of HAp coating for various loading ratios in SBF.

*Corresponding author.
E-mail address: otsuka@vos.nagaokaut.ac.jp (Y. Otsuka).

http://dx.doi.org/10.1016/j.jmbbm.2016.07.026

1. Introduction

Titanium alloys such as Ti–6Al–4V are normally used to implant components due to excellent mechanical properties, corrosion resistance as well as biocompatibility (Niinomi, 1998). In order to achieve tight fixation with optimized load transmission of Ti alloy, implants are coated by hydroxyapatite (HAp) which possesses osteoconductivity and biocompatibility due to its similar chemical composition with the one of human bone. Plasma spraying technique is normally applied to form the HAp coating. HAp coating can promote bone ingrowth around the coating layer and achieve stronger adhesion between human bone with artificial implants (Geesink and Hoefnagels, 1995; Hernandez-Rodriguez et al., 2010). Follow-up results of HAp coated component demonstrate that HAp coated components reduce revision rate and can survive up to 15 years (Palm et al., 2002; Reikers and Gunderson, 2006). Service lives of implant components are required to extend longer than 20 years due to rapid aging in populations. In addition, first operation age of replacement has been lower. These facts suggest that patients are more active and live longer. Both tendencies lead to higher and more frequent loading on fixed implant components. Even though a tight fixation between bone with HAp coating is maintained, delamination between HAp coating with substrate can loose fixations. Reoperation cases have also been reported due to loosening or dislocation of implants that could be attributed to interface fracture of HAp coating (Iwata, 1997; Chung et al., 2009).

In the cases of total jop joints (THPs), mechanisms of fracture are briefly considered as follows:

1. Stress shielding of bone (Niinomi, 2008); much higher Young's modulus of implants metal compared with that of human bone attributes to a reduction in loading allotment in human bone, which leads to an inactivation of bone remodeling process and subsequent reduction in bone density.
2. Loosening of cup or stem part; fracture at interfaces between human bone / HAp coating layer or HAp coating layer / Ti alloy substrate released the fixation forces at the interface, which results in promoting displacement of cup or stem in loading. Causes of interface fracture are summarized as the follows;
   (a) Dissolution of HAp coating by inflammatory reactions; activated macrophages by wear debris dissolve HAp coating layer (Bauer and Schils, 1999)
   (b) Dissolution of HAp coating by body fluid (Grabmann and Heimann, 2000)
   (c) Fatigue fracture at the interfaces due to cyclic loading
3. Final fatigue failure at fixation parts; osteolysis or loosening could lead to stress concentration and fatigue failure of stem components at fixation parts.

In order to extend service lives of THP components, preventive measures for loosening are indispensable. For the mechanism of the loosening, the cause 2(a) chemical dissolution has been considered as primal one. However, recent clinical report demonstrated no evidence of inflammation around a lost part of HAp (Tonino et al., 1999) and pointed out the necessity of considering additional mechanism such as 2(d) mechanical fatigue fracture (Sun et al., 2001; NIH consensus, 1995). Furthermore in ISO standard for durability of stem part (Implants for surgery, 2010), changes in loading state by loosening were not considered. It is necessary to elucidate an interface fatigue fracture mechanism of HAp coating for the purpose of developing more accurate pre-service durability evaluation of THP components.

A stem part of THP components is normally subjected to positive or negative bending/torsional moment during normal walking, squatting down, running or jumping, etc. (T.J.S. (1993)). Amplitudes of loading also vary from 3 to 10 times higher than human's weight according to the human activities. In a finite element stress analysis of THP, stress concentration occurred at a proximal part where an edge of stem contacts with cortical bone (NEDO, 2008). Furthermore, failures of stems also occur at the proximal inside parts due to loosening according to clinical reports of failures (Howell et al., 2004). For the aspect of mechanical properties of plasma-spraying HAp coating, various studies have considered the causes of delamination of HAp coating such as; residual stress (Yang and Chang, 2001; Nimkerdphol et al., 2014), decrease in mechanical strength by thermal decomposition of HAp into TCP (Grabmann and Heimann, 2000), defects by pore or not-melted particles (Khor et al., 2003; Chen et al., 1997). The dissolution of TCP phase in coating by weak-acidity body fluid also decrease the strength of coating. However, for fatigue properties of plasma-sprayed HAp coating, there have been few studies such as AE monitoring for longitudinal cracking process and promotion of cracking by simulated body fluid (Laonapakul et al., 2012, 2012). The authors reported cyclic delamination behavior of plasma-sprayed HAp coating by tensile-compressive loading and demonstrated that interface crack propagation rate followed Paris law (Otsuka et al., 2016). Recent clinical reports suggest that HAp coating may increase a risk of revisions in long-term use (Chung et al., 2009; Lazarinis and Krärholm, 2010). Delamination of HAp coating by cyclic loading can be a cause because it deteriorates fixation of implant components. Therefore, delamination behaviors of HAp coating should be revealed. However, the interaction between loading ratios with dissolutions on cyclic delamination behavior of HAp coating has not been revealed yet though the interaction is an important factor in considering durability of HAp coating.

This study consequently aims at developing a prediction model of cyclic delamination lives of HAp coating by considering a delamination growth mechanism in SBF with interface contact effect by the changes in loading ratios. At first, a comparison between delamination behaviors by static loading with the ones on cyclic loading was conducted in order to show the effect of interface contact. Next cyclic delamination tests of HAp coating in SBF with various stress ratios were conducted in order to reveal the delamination propagation behavior by combined effects of wear with dissolutions. A prediction model for cyclic delamination lives combined by the effects of energy release rates, experimental surface wear and dissolution rate was subsequently developed. A comparison between the predicted results by the

Please cite this article as: Otsuka, Y., et al., Prediction of cyclic delamination lives of plasma-sprayed hydroxyapatite coating on Ti–6Al–4V substrates with considering wear and dissolutions. Journal of the Mechanical Behavior of Biomedical Materials (2016), http://dx.doi.org/10.1016/j.jmbbm.2016.07.026

proposed model with experimental results were finally discussed.

2. Experimental procedure

2.1. Fabrication process of cyclic delamination testing specimen

The test specimen was made of Ti–6Al–4V, which is used normally as an implant substrate material. Tables 1, 2 show the chemical composition and mechanical properties of Ti–6Al–4V, respectively. Fig. 1 shows the microstructure of Ti–6Al–4V that is composed of white α-phase and black β-phase. A NC lathe and a machining center were used to form round bar into the specimen shape as shown in Fig. 2. Specimen surfaces are polished by only from # 800 to # 2000 emery papers in order to keep the sharpness of the edge of square cross section. The specimen was subsequently heat-treated at 923 K for 3.6 ks in an atmospheric electric furnace (MRH-32UHS, Isuzu Manufacturing Co, Ltd., Japan) and air-cooled.

HAp powder (HAP-100, Taihei Chemical Co. Ltd., Japan) was used for plasma-spray. The HAp powder was sintered at 1473 K and 3.6 ks with controlled heating/cooling rate 100 K/h in the atmospheric electric furnace. The sintered HAp powder was subsequently milled by ball milling machine and was put through with a sieve of mesh size 90 μm. Before plasma-spraying, surfaces of Ti substrates were grid-blasted by alumina powders with 5 MPa pressure (Nema blaster, Fujuetsu Manufacturing Co. Ltd., Japan). The grid-blasted substrates were ultrasonically cleaned in acetone solution. The cleaned specimens were subsequently wet-blasted by a slurry of Ti and HAp powders with 0.5 MPa pressure (Macoho Co. Ltd., Japan). The wet-blast process was the same as the one proposed by Rakngarm and Mutoh (2009). Finally, atmospheric plasma spraying was performed by 9MB(Sulzer-metco, Switzerland) with the conditions of 68 V, 500A, spraying distance 140 mm, number of spraying pass 10, respectively. The surface except for spraying area was masked by stainless steel cover to form rectangular coating shape 3×3 mm^2. Target thickness of the HAp coating was 100–150 μm. Bending strength of HAp coating is approximately 250 MPa and tensile strength is 32.2 ± 4.5 MPa (ϕ=25 mm), respectively (Laonapakul et al., 2012; Hakozaki et al., 2016).

Table 1 – Chemical composition of Ti–6Al–4V.

Al	V	H	O	N	C	Fe	Ti
6.42	4.18	0.0063	0.20	0.004	0.016	0.20	Bal.

Table 2 – Mechanical properties of Ti–6Al–4V.

0.2 % proof stress (MPa)	Tensile stress (MPa)	Elongation (%)	Hardness (Hv)
756	799	15	335

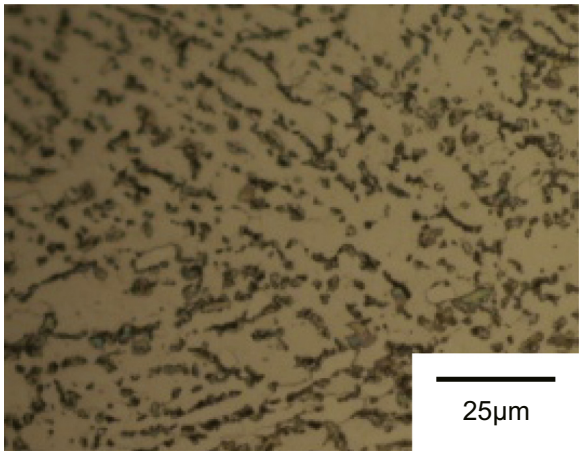

Fig. 1 – Microstructure of Ti–6Al–4V.

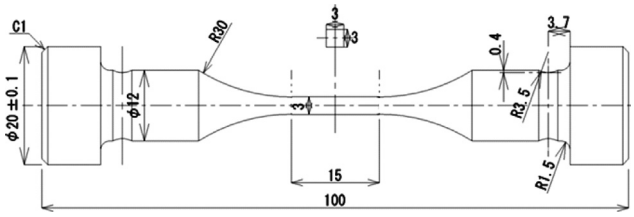

Fig. 2 – Axial fatigue specimen of Ti–6Al–4V for cyclic delamination test of HAp coating. 3×3 mm^2 HAp coating is deposited at the center of testing section 15 mm.

2.2. Cyclic delamination testing condition

Fatigue testing machine (load capacity 30 kN, Shimadzu Co. Ltd., Japan) with water bath and flow circulating system was used. At first static loading tests with maximum stress 400 MPa or −400 MPa were conducted. Though there were no delamination occurred by the static loading and then cyclic loading with the same maximum stress and stress ratio R=0.1 or 10 were applied in order to initiate pre-delamination approximately 100 μm. The delamination propagation behavior by static loading of 400 MPa or −400 MPa were subsequently observed. Cyclic loading tests were conducted by R=0.1, −1 and 10 with loading frequency of 10 Hz. Yoshimoto et. al. conducted FEM analyses of stem parts and they found that maximum stress on the surface of stem part could reach several hundreds MPa (Yoshimoto et al., 2015). Delamination behavior was observed by digital microscope (VHX-1000, Keyence Co. Ltd., Japan). Movies in a single loading cycle were taken at a test stress with f=0.05 Hz. Pictures at maximum loading when delamination paths are the most visible are retrieved from the movies by using an image software in VHX-1000. The cycles of observation was included into total delamination lives. In the cases of comparing cyclic delamination lives of static load tests with those of cyclic load tests, equivalent loading time t_{eq} was used. Cyclic loading time is defined by the cycles when more than 90% of maximum or minimum stresses are applied. Cyclic delamination lives N_f were defined by the periods when delamination length reached 1.2 mm. The definition does not directly mean service lives of implants because the stress

Please cite this article as: Otsuka, Y., et al., Prediction of cyclic delamination lives of plasma-sprayed hydroxyapatite coating on Ti–6Al–4V substrates with considering wear and dissolutions. Journal of the Mechanical Behavior of Biomedical Materials (2016), http://dx.doi.org/10.1016/j.jmbbm.2016.07.026

distributions on the complex surface of implants are not constant. However, if a delamination reached a specific length, the coating partly falls off by cracking at the tip of the delamination. Lost part of coating will result in loosening between human bone with substrates of implants, which will deteriorate service lives of implants. Therefore, our definition of failure lives is important to discuss an integrity of implant components.

Solution used in this study is Kokubo's SBF solution (Kokubo and Takadama, 2006). The temperature of this SBF solution was maintained at 310±1 K by using an incubator and the specimen was immersed in the solution for 7 days in advance. Graßmann and Heimann reported that HAp elution and precipitation reached equilibrium after approximately 7 days (Grabmann and Heimann, 2000) and therefore we decided to use the same period in this study. Nimkerdphol et al. also observed dilution of ACP or another calcium phosphate phases by SBF immersion using XRD and Raman spectroscopy (Nimkerdphol et al., 2014). During cyclic delamination testing, SBF solutions were circulated at controlled temperature 310±1 K. SBF solutions were exchanged every two days in order to keep their initial ion concentrations.

2.3. Observation method at delamination

The side surfaces of HAp coating/Ti substrate were polished by emery papers (from #400 to #2000) and buff polishing with diamond pastes (6–1 μm) in order to detect interface passes clearer. Profiles of polished side surfaces were observed by laser microscope (OLS 4000, Olympus Co. Ltd., Japan) at before/after testing for the purpose of detecting wears at interfaces by cyclic loading. During cyclic delamination testing, delamination behaviors were intermittently observed by long-range digital microscope (VHX-1000, Keyence Co. Ltd., Japan). Delamination passes and tips were subsequently observed by SEM (JSM-6306A, JEOL Ltd., Japan).

2.4. Finite element analyses at delamination regions

Energy release rates G at the tip of delamination were calculated by Virtual Crack Closure Technique (VCCT) by 2D FEA. Young's modulus E and Poisson's ratio ν for both materials are 110 GPa and 0.33 for Ti–6Al–4V and 70 GPa and 0.24 for HAp, respectively. The mechanical properties of coating and substrates were referred to Sun et al. (2001) and Ren et al. (2009). Delaminated coating interface is assumed to be normal contacting which can separate with each other and remained interface in front of crack tip is bonded. Friction coefficient is set to be 0.7 referred by Yugeswaran et al. (2012). Around the crack tip, 1/4 node singular elements are used (Otsuka et al., 2016).

3. Results

3.1. Comparison of delamination behavior between static loading with cyclic loading

Fig. 3 shows the cyclic delamination lives by static loading and by cyclic loading. In the cases of static loading,

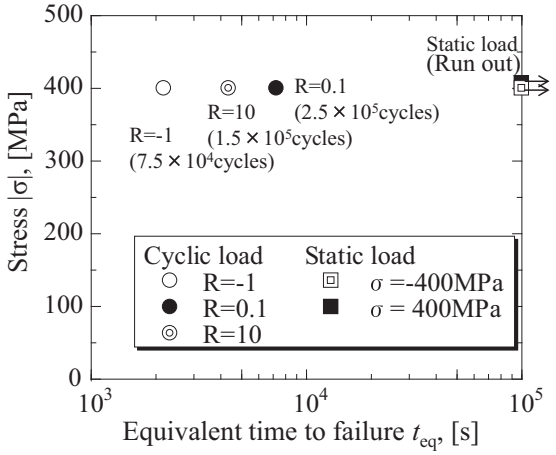

Fig. 3 – Comparison of delamination time between static load cases with cyclic load cases. Equivalent time to failure t_{eq} is defined by the time when delamination length reached 1.2 mm.

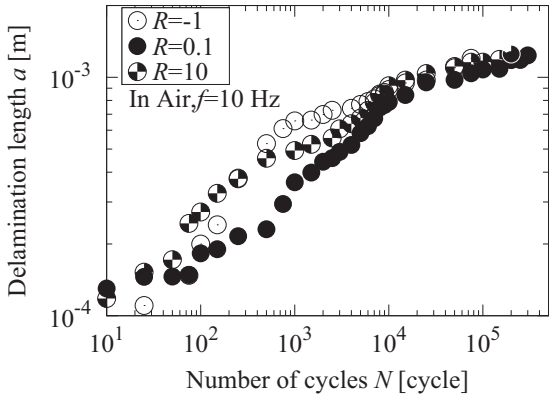

Fig. 4 – Delamination growth history tested at $\sigma_{max} = 400$ MPa, loading frequency $f = 10$ Hz, in air.

delamination was not initiated. On the contrary, cyclic loading generated delaminations of HAp coating at early periods. The cyclic delamination lives became shorter by compression; $R=0.1$ (tension–tension) $>R=10$ (compression–compression) $>R=-1$ (tension–compression). Fig. 4 shows a relationship between delamination length with number of cyclic loading. Initiation lives of delamination were determined by the cycles when delamination of more than 100 μm was observed. The figure demonstrates that initiation lives of delamination are ignorable because the live occupy a period only less than 0.1% in total lives. The immediate initiation behaviors of delamination are due to stress singularity field at the edges of interface. Figs. 5 and 6 show examples of observing delamination paths. Paths from optical images and the one by SEM pictures are nearly matched. Fig. 7 shows the relationship between delamination length with delamination propagation rate. The delamination propagation rate decreases with increasing delamination length for both cases. Though there was no delamination in static loading case, 100 μm pre-delamination was initiated by cyclic loading with the same maximum stress. However, the delamination propagation rates by static loading were much lower than those

Please cite this article as: Otsuka, Y., et al., Prediction of cyclic delamination lives of plasma-sprayed hydroxyapatite coating on Ti–6Al–4V substrates with considering wear and dissolutions. Journal of the Mechanical Behavior of Biomedical Materials (2016), http://dx.doi.org/10.1016/j.jmbbm.2016.07.026

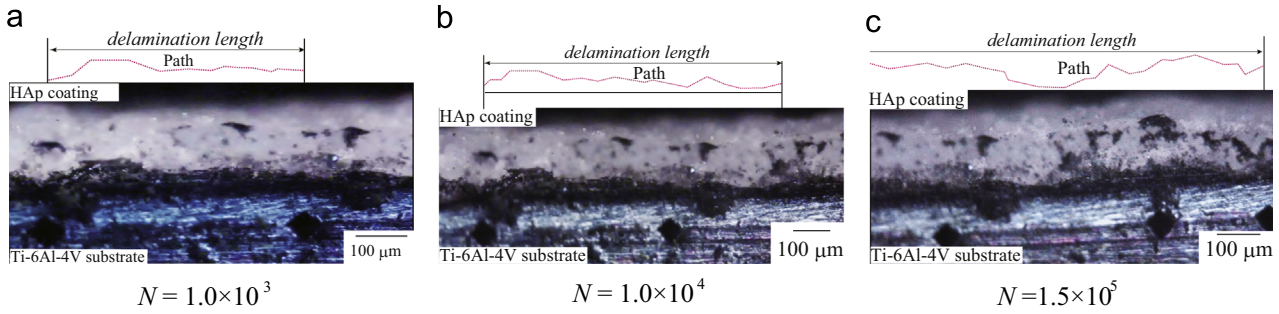

Fig. 5 – Optical images of delamination in the cases of $\sigma_{max} = 400$ MPa, $R = 10$.The pictures are retrieved from movies in a single loading at $f = 0.05$ Hz. Vickers marker are put on the substrate at delamination length $a = 0, 500, 1000, 1200$ μm, respectively. (a) $N = 1.0 \times 10^3$, (b) $N = 1.0 \times 10^4$, (c) $N = 1.5 \times 10^5$.

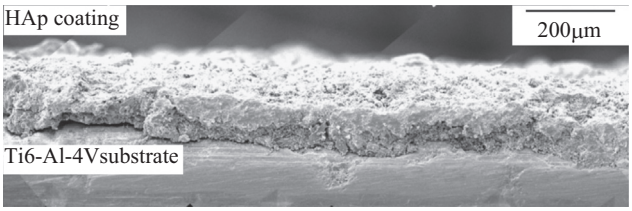

Fig. 6 – SEM image of delamination in the cases of $\sigma_{max} = 400$ MPa, $R = 10$.

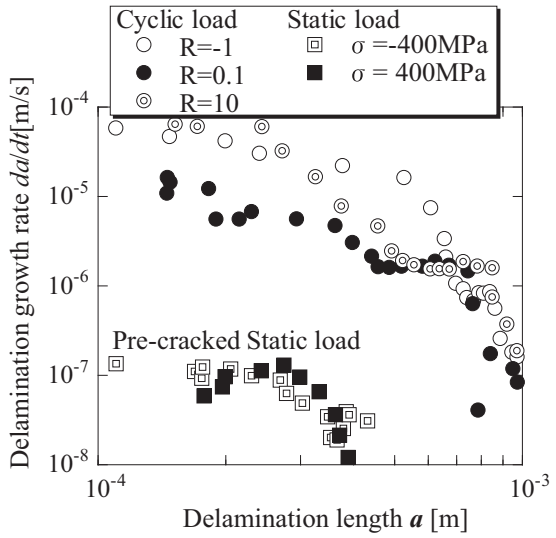

Fig. 7 – Comparison of delamination rate between static load cases with cyclic load cases. In static load cases, pre-cracks were initiated by using cyclic load at same absolute maximum stress levels (400 or −400 MPa) because there were no delaminations by applying static load.

by cyclic loading and the delaminations soon stopped at the length of 400–500 μm. There was no difference in the delamination rates in the cases of tensile static loading or compressive static loading. On the contrary, in the cases of cyclic loading, the delamination propagation rate became higher by the existence of compressive cyclic loading; the delamination rates were higher in the cases of $R = -1, 10$ than that in the case of $R = 0.1$.

Fig. 8 shows the changes in side surface profiles at delamination tip. The profiles were measured at 1200 μm in cyclic loading case and at 500 μm in static loading, respectively.

In Figs. 8(a) $R = -1$, (b) $R = 10$, worn areas were observed. However, there were no worm area in Fig. 8(c) $R = 0.1$, when only tensile loading was applied. Furthermore, Fig. 8 (d) static compressive loading case also showed no worn area. The results demonstrated that cyclic compressive loading promoted wear around delamination tips. Fig. 9 shows slip displacements between HAp coating with substrates. The extents of slip displacement gradually increased with increasing length of delamination. If slip motion and contact force exist, wear behaviors occur at tips of delamination where a boundary of slip and stick behaviors places. In addition, HAp particles are detached by slip displacements because bonding strength among HAp splats are not strong. Therefore, the particles of HAp could be generated by fall-out from HAp coating by slips and then the particles can be regarded as wear debris.

Fig. 10 shows SEM pictures at delamination tip for three loading conditions. There were worn particles in interface and corresponding damaged delamination faces in the cases of compressive loading, as shown in Fig. 10(a) $R = -1$, (b) $R = 10$. Fig. 10 (c) $R = 0.1$ showed no such worn particles at the delamination tip. The size of worn particles distributed from 1 to 30 μm. Fig. 11 shows SEM pictures at delamination tips by static loading. The picture clearly showed no worn particles. Furthermore, there were no perpendicular microcracks in coating layer. Consequently, the evidences of wear were observed only in the cases of cyclic and compressive loading.

3.2. *Cyclic delamination behaviors of HAp coating in SBF*

Fig. 12 shows the relationship between maximum stresses with delamination lives. Delamination lives became shorter in SBF than those in Air. At $\sigma_{max} = 350$ MPa in Air showed no initiation of delamination, whereas delamination reached to 1.2 mm at the same stress level in SBF. The differences among delamination lives at three stress ratios became smaller in SBF. However, the order of delamination lives to the stress ratios still kept the one in Air; $R = 0.1$ (tension–tension) $> R = 10$ (compression–compression) $> R = -1$ (tension–compression). Fig. 13 shows the relationship between delamination length with delamination propagation rate in the cases of $\sigma_{max} = 400$ MPa in Air and $\sigma_{max} = 250$ MPa in SBF. The delamination propagation rates became lower with longer

Please cite this article as: Otsuka, Y., et al., Prediction of cyclic delamination lives of plasma-sprayed hydroxyapatite coating on Ti–6Al–4V substrates with considering wear and dissolutions. Journal of the Mechanical Behavior of Biomedical Materials (2016), http://dx.doi.org/10.1016/j.jmbbm.2016.07.026

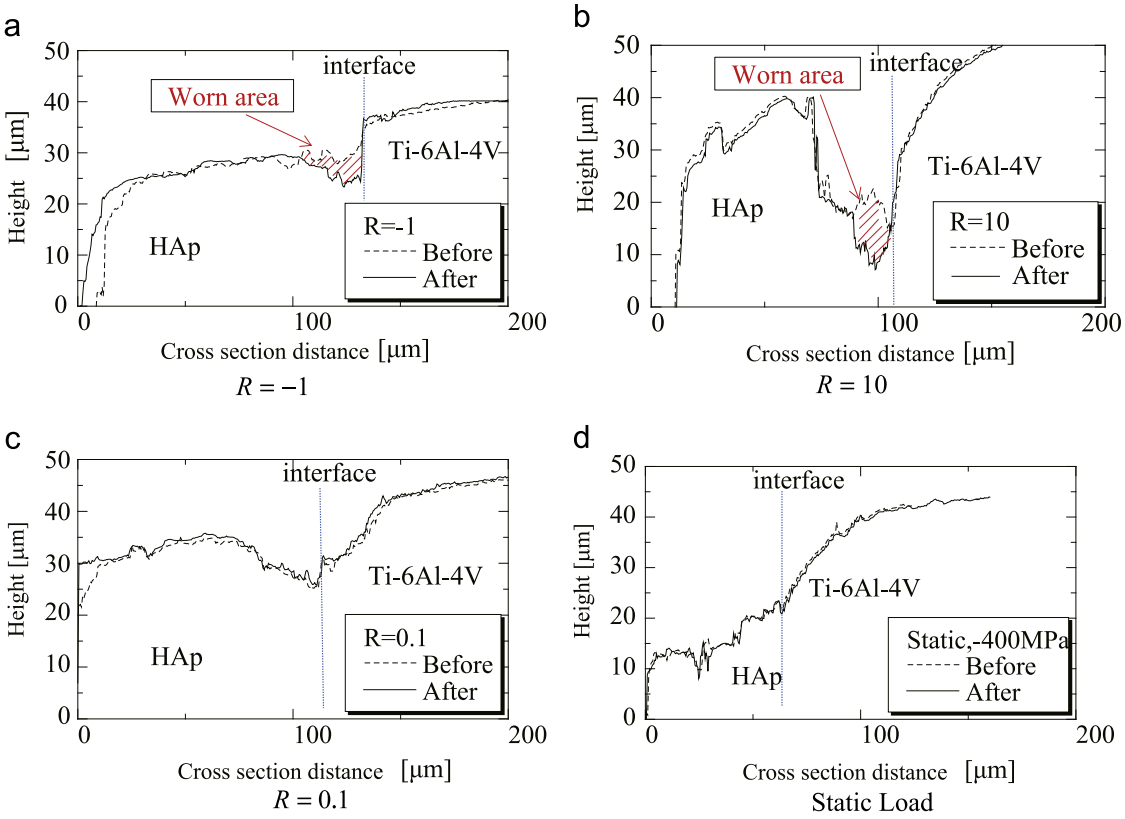

Fig. 8 – Height profile changes after static or cyclic load tests at the delamination tips $a = 1.2$ mm. Cyclic and compressive loading can promote wear at the tips.

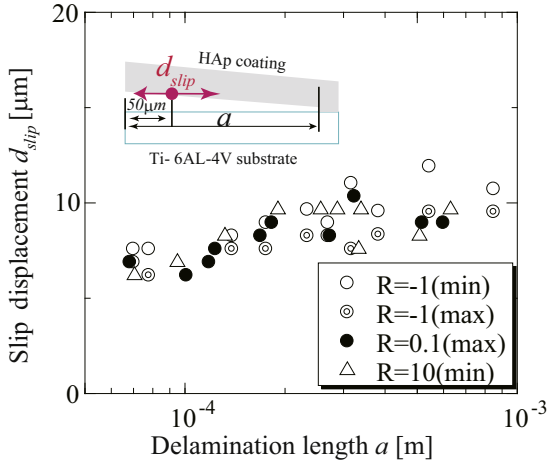

Fig. 9 – Changes in slip displacement d_{slip} at $\sigma_{max} = 400$ MPa, loading frequency $f = 10$ Hz, in air.

delaminations in both environments. The effect of stress ratios on delamination propagation rates decreased in SBF.

Fig. 14 shows SEM pictures of delamination passes in three stress ratio cases. In the case of R=10 in SBF, worn particles were observed in the interface between HAp coating with Ti alloy substrates at the tip of delamination, the same as in the cases of $R = -1$ and $R = 10$ in Air. In contrast, there was no such worn particle in the case of R=0.1 in SBF. Furthermore, edge of delamination pass and delamination tips became round probably due to the effect of dissolution by SBF. In the case of $R = -1$ in SBF, both worn particles inside delamination and round shape at the delamination tip were observed.

4. Discussions

4.1. *Effect of interface contact on delamination propagation*

Once a strong bond between bones with surface of HAp coating are formed, relative displacements at the interface between bones with HAp coating are prevented, which leads to prevention of wears. However, if delamination occurs at an interface between HAp coating with substrate of implants, relative displacements can occur by cyclic loading. In addition, HAp coating on substrates of stem parts or acetabular cups has edge parts which initiate delamination by loading due to stress singularity. Therefore, even though a strong bond between bones with surface of HAp coating would be achieved, HAp coating can initiate delamination by cyclic loading at edge parts of its interface with substrate. Fig. 3 clearly showed the effect of cyclic loading on initiations of delamination at the interface between HAp coating with Ti substrates. The primal difference between static loading and cyclic loading is relative displacement at the interfaces. It is rational to predict that such relative displacements can lead to wears at softer HAp coating layer and promote delamination initiation. According to conventional Archard's equation to determine wear rate (Yamamoto and Kaneta, 2000), wear

Please cite this article as: Otsuka, Y., et al., Prediction of cyclic delamination lives of plasma-sprayed hydroxyapatite coating on Ti–6Al–4V substrates with considering wear and dissolutions. Journal of the Mechanical Behavior of Biomedical Materials (2016), http://dx.doi.org/10.1016/j.jmbbm.2016.07.026

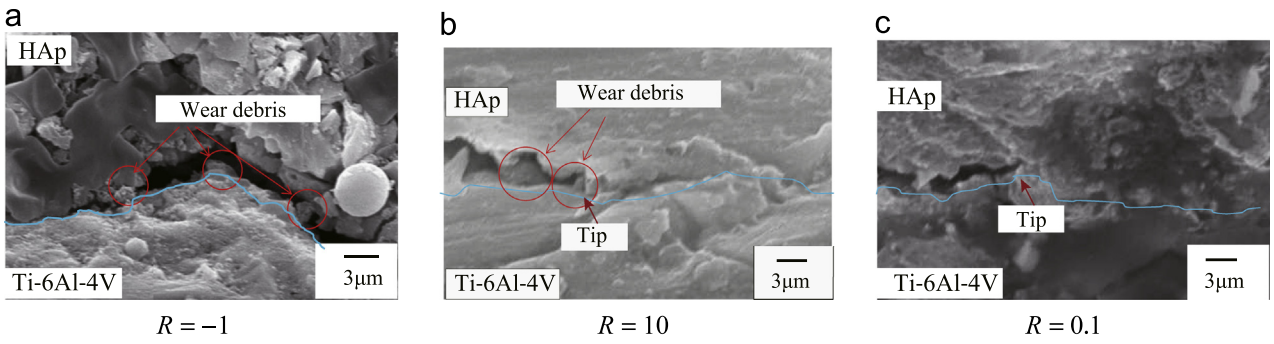

Fig. 10 – SEM pictures for wear debris at delamination tips by cyclic loading. Only in the cases of compressive loading, wear debris were observed.

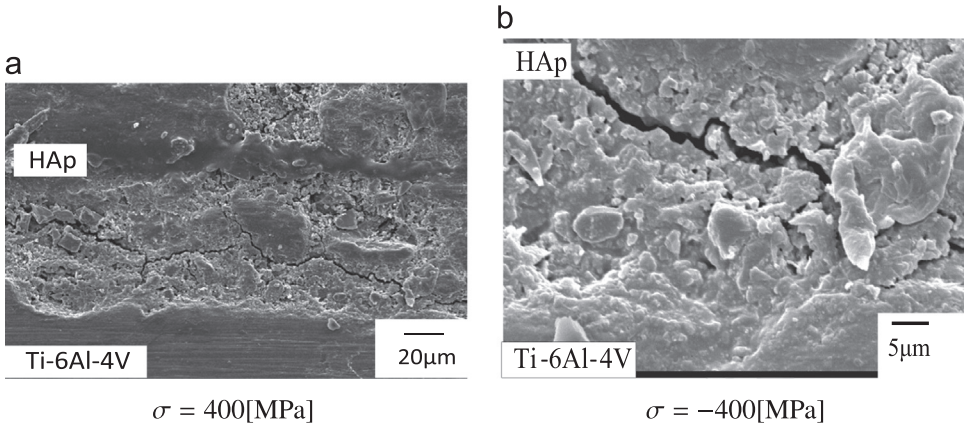

Fig. 11 – SEM pictures for wear debris at delamination tips by static loading. No wear debris were observed.

rate can be determined by the combination of the extent of relative displacement rate and contact normal pressure. The cyclic loading test by $R=-1$ should exhibit the shortest lives where relative displacement is the largest and compressive pressure applied during a half cycle in total loading periods. Cyclic delamination lives by $R=10$ where only compressive pressure applied were placed next. In the case of $R=0.1$, cyclic delamination lives showed the longest due to the absence of both the factors. Such an order in three delamination lives strongly indicated the significant effect of wear by interface contact on total cyclic delamination lives.

Figs. 8 and 10 showed that worn particles were HAp because HAp coating is softer than Ti substrates due to the existence of particle boundary of molten splats, cracking or porosities. HAp coating was mainly worn by its contact to Ti substrate during loading, which generated worn particles in the space between their surfaces. The mechanism is explained by normal abrasive wear. Furthermore, Fig. 10 showed that worn particles reached to the vicinity of delamination tips. Promotion mechanism in delamination by wear at tips can be considered as follows;

1. Third body effect of wearing Worn particles were transported into newly formed delamination part by relative displacement, which could promote delaminations at new tips.

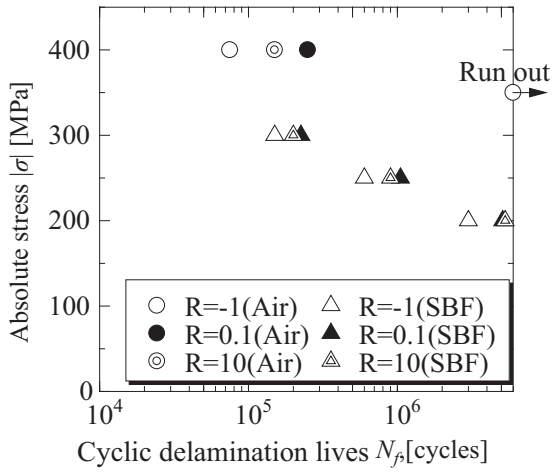

Fig. 12 – Effects of SBF solutions and loading ratio on cyclic delamination lives of HAp coating.

2. Worn-particle-assisted crack opening Inserted worn particle forced to open delamination even in the cases of compressive loading, which could increase mean value of mode I stress intensity factor (K_I) during loading. Because cracks in ceramics are normally propagated by integrated time with maximum stress intensity factor and then the increase in mean K_I should promote delaminations.

Please cite this article as: Otsuka, Y., et al., Prediction of cyclic delamination lives of plasma-sprayed hydroxyapatite coating on Ti–6Al–4V substrates with considering wear and dissolutions. Journal of the Mechanical Behavior of Biomedical Materials (2016), http://dx.doi.org/10.1016/j.jmbbm.2016.07.026

Kida and Ogura (1999) observed the latter mechanism in Mode III cracking of bearing ceramics with contact fatigue conditions. Kaneta et al. (1985) also discussed the effect of crack opening by filtrated oils in fatigue behaviors of steels in oil environment. Their result could support the above discussion that worn particles or SBF also promoted delamination propagations in the same manner.

4.2. *Effect of SBF in promoting delamination propagation*

SBF also assisted delamination propagations for both positive and negative stress ratios by chemical dissolutions at coating layers. SBF dissolved HAp coating layers which contains thermally decomposed phases such as ACP or TCP (Grabmann and Heimann, 2000). Chemical dissolution at delamination tips would generate pores, weakened bonding between coating layer and substrate or crevice corrosion. All causes could accelerate delaminations. In case of $R=-1$, dissolution effect primarily promoted delamination propagation. In addition in the cases of $R=-1$ and $R=10$, combined effect of wear and dissolution attacked coating layer. However, friction coefficient between HAp coating and Ti substrate would become lower in SBF because of lubrication effect of the fluid, which lead to smaller variations in total cyclic delamination lives among three stress ratios.

4.3. *Applicability of Paris law to predict delamination lives*

Energy release rates G at delamination tips were calculated by FEA (Otsuka et al., 2016). Fig. 15 shows the effects of friction on the ratio of G_I/G_{II}. G_{II} became higher when friction was considered. Yuuki et al. conducted Boundary Element method (BEM) for a lap shear joint (Yuuki, 1993; Yuuki et al., 1992). They observed that G was independent from a ratio of delamination length to total bonding length. In present FEM results, G slightly decreased with increasing the delamination length, especially in the cases of compressive loading probably due to friction effects between delamination faces at delamination tips. Tanaka et. al. experimentally observed such a stress shielding effect in effective stress intensity factor range in mode III loading conditions (Tanaka et al., 1997). Consequently, we used G_{max} value by FEM, which has negative correlations with delamination length, in arranging Paris law curves.

Fig. 16 shows the effects of SBF immersion on delamination growth curve of HAp coating. Considering G_{max} by FEM results can arrange normal Paris law curves. However, the curves in different environment is not overlapped. The results suggest that wearing rate and dissolution rate are

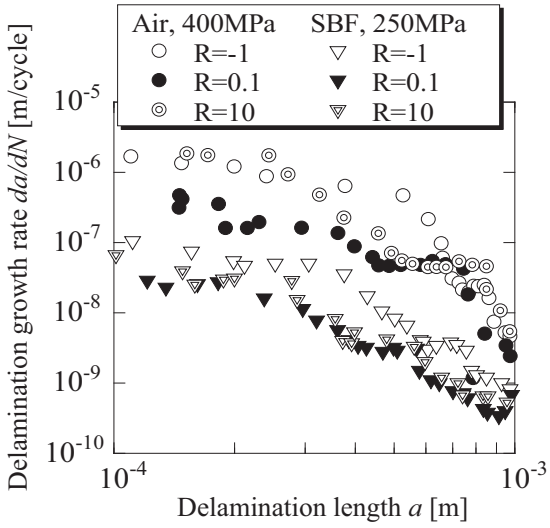

Fig. 13 – Relationship between delamination growth rates with delamination length in both environments.

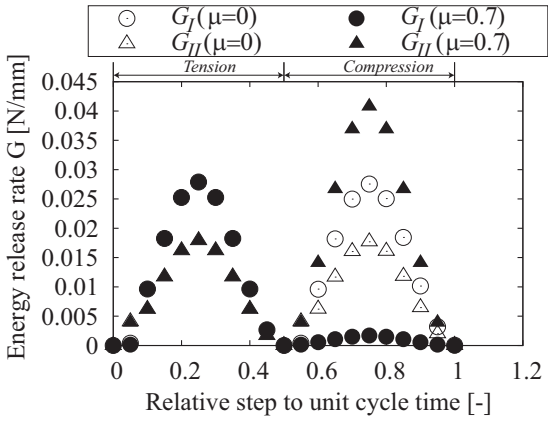

Fig. 15 – Effects of friction coefficient μ on the ratio of energy release rate $\frac{G_{II}}{G_I}$ in $R=-1$ loading.

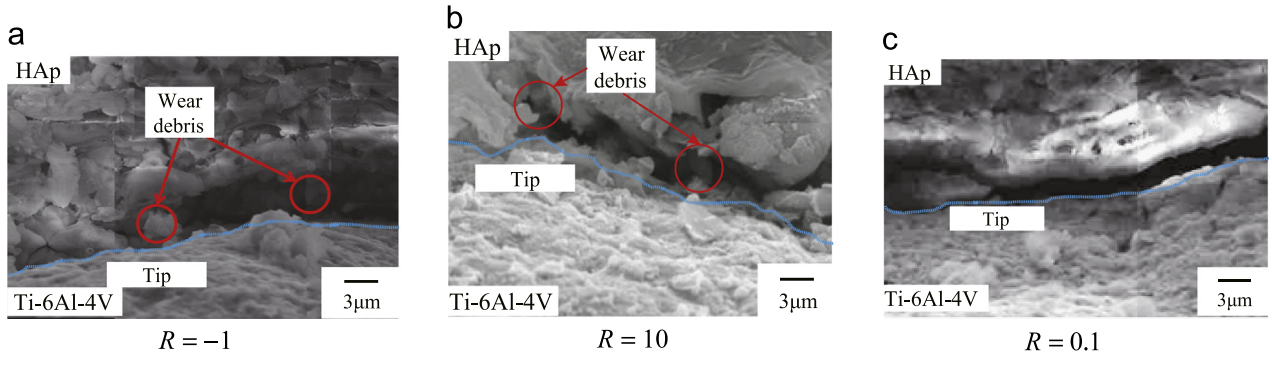

Fig. 14 – SEM pictures for wear debris at delamination tips by cyclic loading tested in SBF. Delamination width became larger by dissolution in SBF.

Please cite this article as: Otsuka, Y., et al., Prediction of cyclic delamination lives of plasma-sprayed hydroxyapatite coating on Ti–6Al–4V substrates with considering wear and dissolutions. Journal of the Mechanical Behavior of Biomedical Materials (2016), http://dx.doi.org/10.1016/j.jmbbm.2016.07.026

stress-dependent. We then considered a different prediction model for cyclic delamination lives by including both the effects of wear and dissolutions. At first wear rates κ is calculated by the following process.

1. Wear rate for the cases of cyclic delamination testing at R=0.1 is considered to be zero because interface contact during loading can be negligible.
2. Differences between cyclic delamination lives of R=0.1 (without contact) with the one of R=10 (with contact) can be attributed to wear effect $\kappa \times N_{f,R=10}$.
3. Stress-dependent wear rate κ can then be calculated by using Eq. (1).
4. The calculations are conducted to both tested data in Air and the ones in SBF because friction coefficient in SBF should be different from the one in Air.

$$\kappa = \frac{a_{f,R=10} - a_{R=0.1}}{N_{f,R=10}}$$

$$a_{f,R=0.1} = C\int_0^{N_{f,R=10}} G_{max}^m dN \quad (1)$$

κ wear rate [m/cycle]

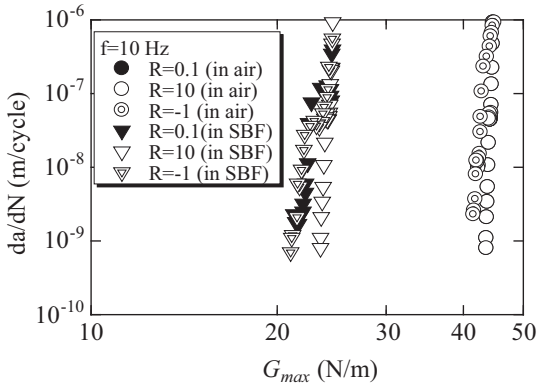

Fig. 16 – Paris law curves of cyclic delamination behaviors of HAp coating.

C,m Paris law coefficient and multiplier at R=0.1 in Fig. 16

$a_{f,R=10}$ final delamination length tested at R=10 (=1.2 mm)

$N_{f,R=10}$ experimental cyclic delamination lives tested at R = 10 shown in Fig. 12

$a_{R=0.1}$ predicted delamination length contributed only by Paris law

Next, dissolution rate ϕ can be calculated by the following similar process.

1. Dissolution rate ϕ for the cases of cyclic delamination data tested in Air is considered to be zero.
2. Differences between cyclic delamination lives tested in Air with the one tested in SBF can be attributed to dissolution effect $\frac{\phi}{f} \times N_{f,SBF}$.
3. Stress-dependent dissolution rate ϕ can then be calculated by using Eq. (2).
4. The calculations were conducted for three stress ratio cases.

$$\phi = \frac{a_{f,SBF} - a_{Air}}{N_{f,SBF}} \times f \quad (2)$$

$$a_{,Air} = C\int_0^{N_{f,SBF}} G_{max}^m dN$$

ϕ dissolution rate (m/s)

f loading frequency (Hz (cycles/s))

$a_{f,SBF}$ final delamination length tested in SBF (1.2 mm)

$N_{f,SBF}$ experimental cyclic delamination lives tested in SBF shown in Fig. 16

a_{Air} predicted delamination length contributed only by Paris law

Table 3 shows the calculated wear rates κ and dissolution rates ϕ. Both rates increase with increasing stress. Yugeswaran et al. (2012) conducted pin-on-disc wear test of gas tunnel type plasma -sprayed HAp coating in SBF and electrochemical test of HAp coating and they obtained sliding

Table 3 – Calculated wear rates κ and dissolution rates ϕ by using Eqs. (1) and (2).

σ_{max} (MPa)	R (–)	$\kappa(\times 10^{-10})$ (m/cycle)	$\phi(\times 10^{-10})$ (m/s)	σ_{max} (MPa)	R (–)	$\kappa(\times 10^{-10})$ (m/cycle)	$\phi(\times 10^{-10})$ (m/s)
400	−1	9.8	0	300	−1	7.4	47
(Air)	10	5.3	0	(SBF)	10	4	5
	0.1	0	0		0.1	0	47
300	−1	9.8	0	250	−1	6.1	39
(Air)	10	5.3	0	(SBF)	10	3.3	4.2
	0.1				0.1	0	39
				200	−1	4.9	31
				(SBF)	10	2.7	3.3
					0.1	0	31

Please cite this article as: Otsuka, Y., et al., Prediction of cyclic delamination lives of plasma-sprayed hydroxyapatite coating on Ti–6Al–4V substrates with considering wear and dissolutions. Journal of the Mechanical Behavior of Biomedical Materials (2016), http://dx.doi.org/10.1016/j.jmbbm.2016.07.026

wear rate $1.8 \sim 2.7 \times 10^{-8}$(mm^3/Nmm) and $\phi = 1.2 \times 10^{-10}$(ms). Archard specific wear rate can be calculated by the following equation:

$$\kappa_{arc} = \frac{\kappa \times W_{area}}{P_{contact} \times D_{slide}} \quad (3)$$

κ_{arc}	archard specific wear rate (mm^3/Nmm)
κ	wear rate for delamination extension
W_{area}	wear area at delamination tip assumed to be $10^{-3} \times 10^{-3}$ mm^2
$P_{contact}$	contact normal force at delamination tips obtained by FEA results (N)
D_{slide}	relative displacement at delamination tips obtained by FEA results (mm)

In case of $\sigma_{max} = 400$ (MPa) in Air, where $\kappa = 9.8 \times 10^{-7}$(mm), $P_{contact} = 2.9 \times 10^{-4}$(N) and $D_{slide} = 3.4 \times 10^{-3}$(mm), κ_{arc} can be estimated 1×10^{-6}(mm^3/N mm). The obtained κ_{arc} was higher than those by Yugeswaran et al. due to weaker microstructure of HAp coating by different spraying method or assumed $P_{contact}, D_{slide}$ by FEA. In order to obtain more accurate wear rate at delamination tips, further observation is necessary. The dissolution rates ϕ were also higher than those by Yugeswaran et al. due to more higher amount of soluble phases such as ACP or TCP in HAp coating. HAp coating made by plasma spraying process contains ACP or TCP phases (Grabmann and Heimann, 2000). In addition, the dissolution in interface can be promoted by crevice corrosion, which leads to higher ϕ in the present study. Consequently, the estimation method by Eqs. (1) and (2) is applicable in later discussions to predict cyclic delamination lives because the differences in the calculated values can be explained by the differences in microstructure.

Cyclic delamination lives prediction model by fracture mechanics parameter with dissolution and wear is shown by the following equations:

$$\text{Only fracture mechanics model } \frac{da}{dN} = C(G_{max})^m \quad (4)$$

$$\text{With wear, dissolution model } \frac{da}{dN} = C(G_{max})^m + \kappa + \phi/f \quad (5)$$

Eqs. (4) and (5) are numerically integrated and the comparisons of predicted delamination lives $N_{f,pre}$ with the experimental ones $N_{f,exp}$ are shown in Fig. 17. Fig. 17 demonstrated that fracture mechanics model with linear combination of wear and dissolution can provide reliable delamination lives estimation. In order to obtain more accurate estimation, interactions between wear and dissolution in solutions may be necessary to be considered. Furthermore, fretting wear at the interfaces between HAp coating layer / Ti alloy substrate (Howell et al., 2004; Yu et al., 2005) should be observed whether it can provide wear debris to contact parts of joints or deteriorate fixation conditions of human bone with HAp coating.

Delamination behavior is occurred in specific cases of coating type and thickness. In the cases of thinner thickness or functionally graded coating, delamination propagates not at interfaces but within coating layers. In the cases, delamination behavior may be affected by microstructural features such as porosity, residual stress, interface morphologies or mechanical properties of the coating layers. In order to widen application of the proposal by this study, damage or fracture process of more practical coating components of load-bearing implants are needed to be observed.

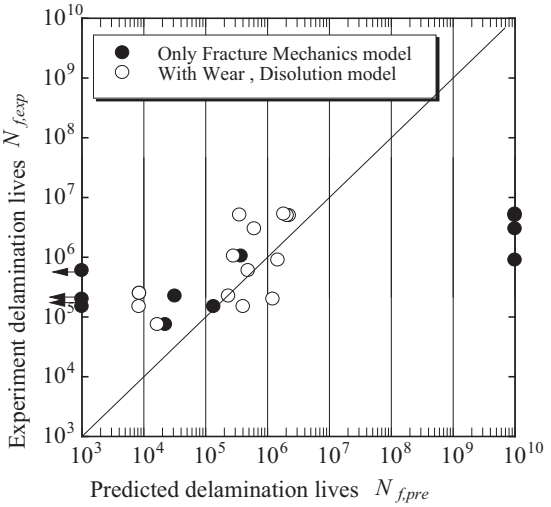

Fig. 17 – Comparison of predicted delamination lives by Eqns. 4 and 5 with experimental delamination lives.

5. Conclusions

This study conducted cyclic delamination tests of plasma-sprayed HAp coating at three different stress ratios in SBF in order to reveal the effects of interface contact and dissolutions on delamination lives of the HAp coating. Summary of the results is as follows;

1. Cyclic loading accelerates initiations and propagations of delamination of plasma-sprayed HAp coating. Delamination lives by cyclic loading is shorter than one tenth of the ones by static loading.
2. Delamination growth rate in compressive–compressive loading in Air was higher than the one in tensile–tensile loading due to wear effect at delamination tips by interface contact. Such acceleration effect was softened in SBF due to decreases in friction coefficient by liquids.
3. SEM observation revealed the existence of wear debris at delamination tips only in the cases of compressive loading. The acceleration effects of wear on delamination can be explained by interface contact (abrasive wear) and intrusion of wear debris into the delamination tips (third body abrasive wear).
4. Fracture mechanics model with linear combination of wear and dissolution can provide reliable delamination lives estimation.

This study revealed that cyclic delamination lives of HAp coating *in vivo* can be predicted by fracture mechanics model with wear and dissolution effects. In order to provide more accurate prediction, interactions among delamination, wear and dissolutions will be considered in details.

Please cite this article as: Otsuka, Y., et al., Prediction of cyclic delamination lives of plasma-sprayed hydroxyapatite coating on Ti–6Al–4V substrates with considering wear and dissolutions. Journal of the Mechanical Behavior of Biomedical Materials (2016), http://dx.doi.org/10.1016/j.jmbbm.2016.07.026

Acknowledgments

The author (Y.O.) was partly supported by the Top Runner Incubation System through the Academia-Industry Fusion Training in the Promotion of Independent Research Environment for Young Researchers, MEXT, Japan. This work was partly supported by JSPS KAKENHI Grant Number 26870213. We greatly appreciate Niigata Metallicon Co. Ltd. for making plasma-sprayed samples. The authors also appreciate the critical advice from Assoc. Prof. Yukio Miyashita at Nagaoka University of Technology.

REFERENCES

Bauer, T., Schils, J., 1999. The pathology of total joint arthroplasty II. Mechanisms of implant failure. Skelet. Radiol. 28 (9), 483–497.

Chen, J., Tong, W., Cao, Y., Feng, J., Zhang, X., 1997. Effect of atmosphere on phase transformation in plasma-sprayed hydroxyapatite coatings during heat treatment. J. Biomed. Mater. Res. 34 (1), 15–20.

Chung, Y.-Y., Ki, S.-C., So, K.-Y., Kim, D.-H., Park, K., Lee, Y., 2009. High revision rate of hydroxyapatite-coated abg-i prosthesis. J. Orthop. Sci. 14 (5), 543–547.

Geesink, R., Hoefnagels, N., 1995. Six-year results of hydroxyapatite-coated total hip replacement. J. Bone Jt. Surg. Ser. B 77 (4), 534–547.

Grabmann, O., Heimann, R.B., 2000. Compositional and microstructural changes of engineered plasma-sprayed hydroxyapatite coatings on Ti6Al4V substrates during incubation in protein-free simulated body fluid. J. Biomed. Mater. Res. 53 (6), 685–693.

Hakozaki, Y., Otsuka, Y., Miyashita, Y., Mutoh, Y., 2016. Effects of adhesives on interfacial strength of plasma-sprayed hydroxyapatite coating. In: Proceedings of APCFS2016, Toyama, Japan.

Hernandez-Rodriguez, M., Ortega-Saenz, J., Contreras-Hernandez, G., 2010. Failure analysis of a total hip prosthesis implanted in active patient. J. Mech. Behav. Biomed. Mater. 3 (8), 619–622.

Howell, J., Blunt, L., Doyle, C., Hooper, R., Lee, A., Ling, R., 2004. In vivo surface wear mechanisms of femoral components of cemented total hip arthroplasties: the influence of wear mechanism on clinical outcome. J. Arthroplast. 19 (1), 88–101.

Implants for surgery—partial and total hip joint prostheses—Part 4: Determination of endurance properties and performance of stemmed femoral components, ISO 7206-4:2010.

Iwata, H., 1997. Basic knowledge and clinical cases of loosing of total hip joint (thp). J. Jpn. Orthop. Surg. Soc. 71 (3), S287.

Kaneta, M., Yatsuzuka, H., Murakami, Y., 1985. Analysis of surface cracking in lubricated rolling contact: crack growth modes and effects of surface traction. Trans. Jpn. Soc. Mech. Eng. Ser. C 51 (470), 2618–2626.

Khor, K., Gu, Y., Quek, C., Cheang, P., 2003. Plasma spraying of functionally graded hydroxyapatite/Ti-6Al4V coatings. Surf. Coat. Technol. 168 (2–3), 195–201.

Kida, K., Ogura, K., 1999. Observations of surface crack growth and wear in Si_3N_4 under ball-on-plate contact. Trans. Jpn. Soc. Mech. Eng. Ser. A 65 (632), 846–852.

Kokubo, T., Takadama, H., 2006. How useful is {SBF} in predicting in vivo bone bioactivity?. Biomaterials 27 (15), 2907–2915.

Laonapakul, T., Otsuka, Y., Nimkerdphol, A., Mutoh, Y., 2012. Acoustic emission and fatigue damage induced in plasma-sprayed hydroxyapatite coating layers. J. Mech. Behav. Biomed. Mater. 8, 123–133.

Laonapakul, T., Nimkerdphol, A.R., Otsuka, Y., Mutoh, Y., 2012. Failure behavior of plasma-sprayed {HAp} coating on commercially pure titanium substrate in simulated body fluid (sbf) under bending load. J. Mech. Behav. Biomed. Mater. 15, 153–166.

Lazarinis, S., Krärholm, J., 2010. N. Hailer, Increased risk of revision of acetabular cups coated with hydroxyapatite: a Swedish hip arthroplasty register study involving 8,043 total hip replacements. Acta Orthop. 81 (1), 53–59.

NEDO, Technology assessment technology of bio-compatibility implant material (in Japanese), NEDO, 2008.

NIH Consensus Conference: Total hip replacement. NIH consensus development panel on total hip replacement. J. Am. Med. Assoc. 273 (24) (1995) 1950–1956.

Niinomi, M., 1998. Mechanical properties of biomedical titanium alloys. Mater. Sci. Eng. A 243 (1–2), 231–236.

Niinomi, M., 2008. Mechanical biocompatibilities of titanium alloys for biomedical applications. J. Mech. Behav. Biomed. Mater. 1 (1), 30–42.

Nimkerdphol, A.R., Otsuka, Y., Mutoh, Y., 2014. Effect of dissolution/precipitation on the residual stress redistribution of plasma-sprayed hydroxyapatite coating on titanium substrate in simulated body fluid (sbf). J. Mech. Behav. Biomed. Mater. 36, 98–108.

Otsuka, Y., Kawaguchi, H., Mutoh, Y., 2016. Cyclic delamination behavior of plasma-sprayed hydroxyapatite coating on Ti–6Al–4V substrates in simulated body fluid. Mater. Sci. Eng. C 67, 533–541.

Palm, L., Jacobsson, S.-A., Ivarsson, I., 2002. Hydroxyapatite coating improves 8-to-10–year performance of the link {RS} cementless femoral stem. J. Arthroplast. 17 (2), 172–175.

Rakngarm, A., Mutoh, Y., 2009. Characterization and fatigue damage of plasma sprayed {HAp} top coat with Ti and HAp/Ti bond coat layers on commercially pure titanium substrate. J. Mech. Behav. Biomed. Mater. 2 (5), 444–453.

Reikers, O., Gunderson, R.B., 2006. Long-term results of ha coated threaded versus ha coated hemispheric press fit cups: 287 hips followed for 11 to 16 years. Arch. Orthop. Trauma Surg. 126, 503–508.

Ren, F., Case, E., Morrison, A., Tafesse, M., Baumann, M., 2009. Resonant ultrasound spectroscopy measurement of Young's modulus, shear modulus and Poisson's ratio as a function of porosity for alumina and hydroxyapatite. Phil. Mag. 89 (14), 1163–1182.

Sun, L., Berndt, C.C., Gross, K.A., Kucuk, A., 2001. Material fundamentals and clinical performance of plasma-sprayed hydroxyapatite coatings: a review. J. Biomed. Mater. Res. 58 (5), 570–592.

T.J.S. of Mechanical Engineers ed., Biomechanics (in Japanese), The Japan Society of Mechanical Engineers, 1993.

Tanaka, K., Akiniwa, Y., Yu, H., 1997. Near-threshold fatigue crack propagation under mode iii torsional loading. Trans. Jpn. Soc. Mech. Eng. Ser. A 63 (612), 1627–1633.

Tonino, A., Thrin, M., Doyle, C., 1999. Hydroxyapatite-coated femoral stems. J. Bone Jt. Surg. Ser. B 81 (1), 148–154.

Yamamoto, Y., Kaneta, M., 2000. Tribology, 2nd Ed. (in Japanese), Rikougakusya.

Yang, Y., Chang, E., 2001. Influence of residual stress on bonding strength and fracture of plasma-sprayed hydroxyapatite coatings on Ti-6Al-4V substrate. Biomaterials 22 (13), 1827–1836.

Yoshimoto, K., Nakashima, Y., Nakamura, A., Mawatari, T., Todo, M., Hara, D., Iwamoto, Y., 2015. Neck fracture of femoral stems with a sharp slot at the neck: biomechanical analysis. J. Orthop. Sci. 20 (5), 881–887.

Please cite this article as: Otsuka, Y., et al., Prediction of cyclic delamination lives of plasma-sprayed hydroxyapatite coating on Ti–6Al–4V substrates with considering wear and dissolutions. Journal of the Mechanical Behavior of Biomedical Materials (2016), http://dx.doi.org/10.1016/j.jmbbm.2016.07.026

Yu, H., Cai, Z., Zhou, Z., Zhu, M., 2005. Fretting behavior of cortical bone against titanium and its alloy. Wear 259 (7–12), 910–918.
Yugeswaran, S., Yoganand, C., Kobayashi, A., Paraskevopoulos, K., Subramanian, B., 2012. Mechanical properties, electrochemical corrosion and in-vitro bioactivity of yttria stabilized zirconia reinforced hydroxyapatite coatings prepared by gas tunnel type plasma spraying. J. Mech. Behav. Biomed. Mater. 9, 22–33.
Yuuki, R., Liu, J.-Q., Xu, J.-O., Ohira, T., Ono, T., 1992. Evaluation of the fatigue strength of adhesive joints based on interfacial fracture mechanics. J. Soc. Mater. Sci., Jpn. 41 (467), 1299–1304.
Yuuki, R., 1993. Mechanics of Interface (in Japanese), Baihuukan.

Please cite this article as: Otsuka, Y., et al., Prediction of cyclic delamination lives of plasma-sprayed hydroxyapatite coating on Ti–6Al–4V substrates with considering wear and dissolutions. Journal of the Mechanical Behavior of Biomedical Materials (2016), http://dx.doi.org/10.1016/j.jmbbm.2016.07.026